Chapter 4
The Heart

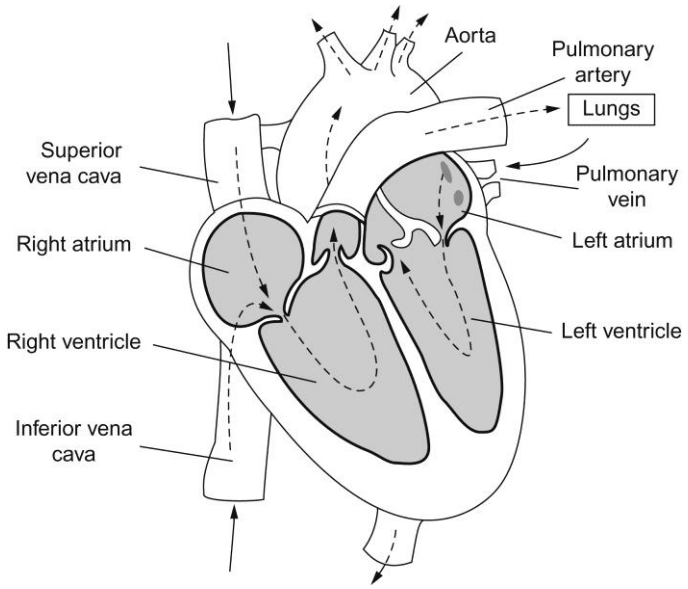

Figure 4.1 Anatomy of the heart depicting the direction of blood flow through the four heart chambers. The right side of the heart collects deoxygenated blood from the systemic circulation and delivers it to the pulmonary circulation. The left side of the heart collects oxygenated blood from the pulmonary circulation and delivers it to the systemic circulation.

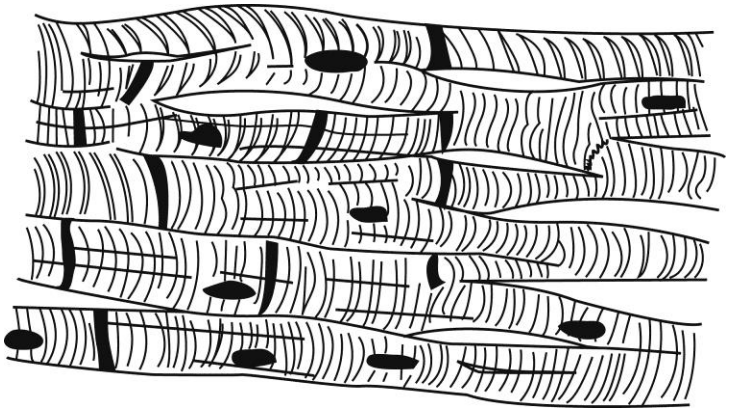

Figure 4.2 Schematic of cardiac muscle cells depicting the highly interconnected fibers that form a syncytium, and the intercalated discs that divide individual muscle cells. There are many gap junctions present within the intercalated discs to facilitate the movement of ions between cells, thus allowing the action potential to continuously flow from one cell to the next. *Source: Adapted from Guyton and Hall (2000)*.

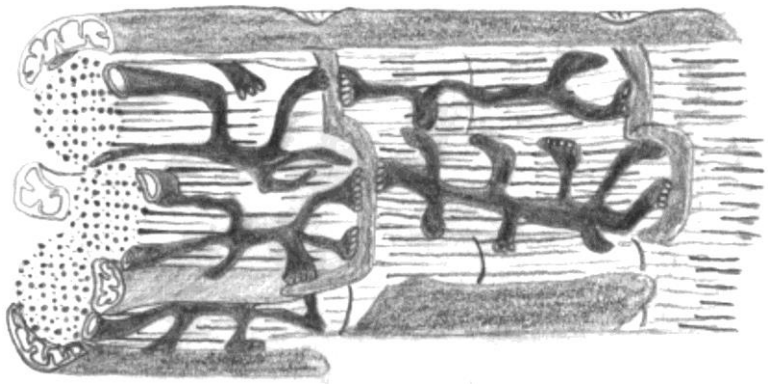

Figure 4.3 Spatial organization of the cardiomyocyte T-tubule system and sarcoplasmic reticulum. Invaginations of the sarcolemma for the T-tubule system, which associates with the sarcoplasmic reticulum at the dyad. *Source: Adapted from Feher (2012)*.

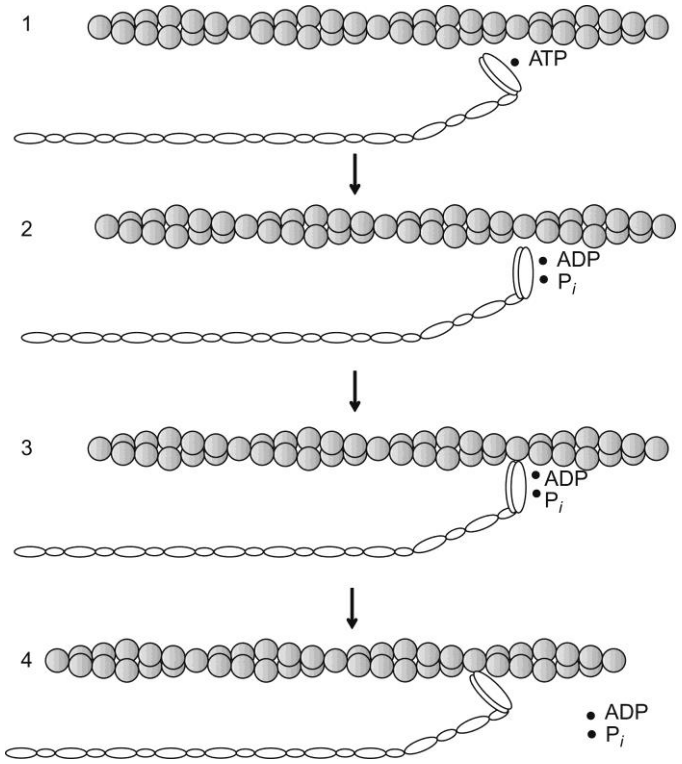

Figure 4.4 Schematic of the actin–myosin cross-bridge cycle. Note that troponin and tropomyosin are not depicted on this figure. (1) ATP binds to myosin, lowering the binding affinity between myosin and actin. (2) ATP is hydrolyzed into ADP and inorganic phosphate. Myosin head alters its conformation and stays in a "ready"•state. In the absence of calcium the cycle will stop here. (3) In the presence of calcium, tropomyosin does not block the myosin binding site of actin and thus an actin–myosin cross-bridge is formed. (4) ADP and inorganic phosphate are released from the myosin head inducing a conformation change of myosin. This conformation change forces actin to move relative to myosin in a process termed the power stroke. In the absence of ATP, the cycle ends here (this is termed rigor).

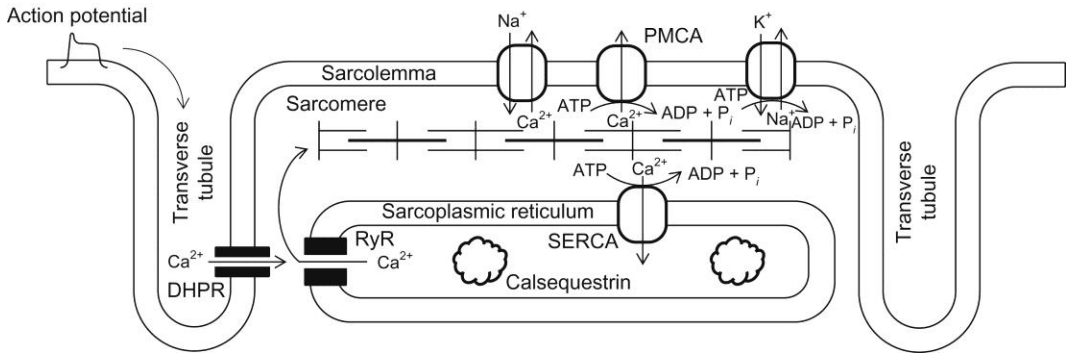

Figure 4.5 Overview of calcium-induced calcium release within cardiac muscle cells. First an action potential passes along the sarcolemma into the transverse tubule system. The action potential induces the opening of the DHPR, which allows a small amount of calcium into the muscle cell. This calcium induces the opening of the RyR found on the sarcoplasmic reticulum membrane, significantly increasing the cytosolic calcium concentration. This calcium is used to regulate cross-bridge formation (depicted in Figure 4.4). Calcium is then taken up by the SERCA to be stored in the sarcoplasmic reticulum and by the sodium calcium exchanger and PMCA on the sarcolemma.

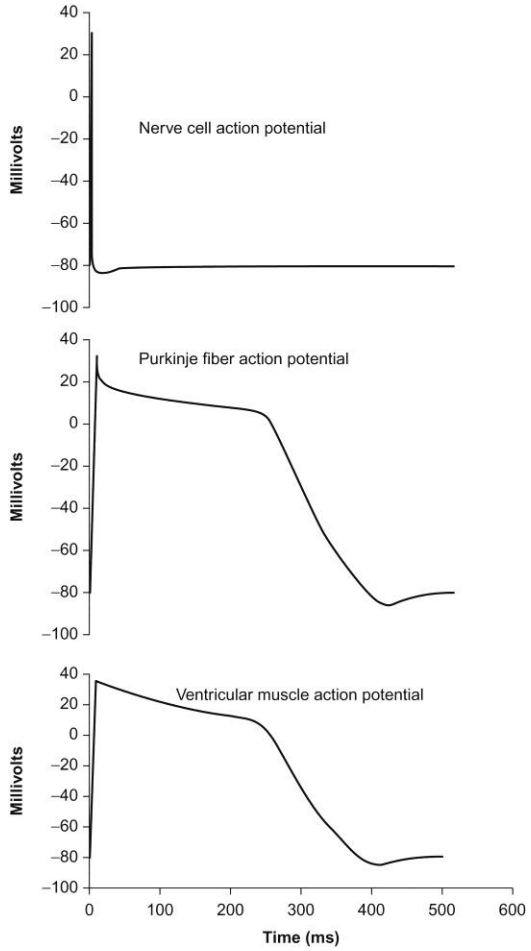

Figure 4.6 Comparison of the action potentials in nervous tissue and cardiac tissue. There is a significant elongation of the depolarization phase in cardiac tissues. Note that the cardiac action potential varies slightly based on what cardiac chamber the myocytes reside and that the myocytes of the SA node have a somewhat significantly different action potential waveform.

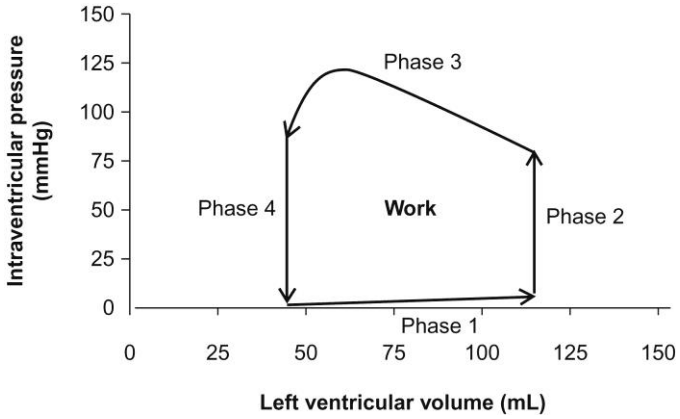

Figure 4.7 The pressure–volume relationship for the left ventricle, which describes the work that the left ventricle conducts. The work is the area within the pressure–volume curve. The work the heart conducts can drastically change under disease conditions. Note that work associated with the acceleration of blood is ignored on this figure and within the analysis of work conducted by the heart.

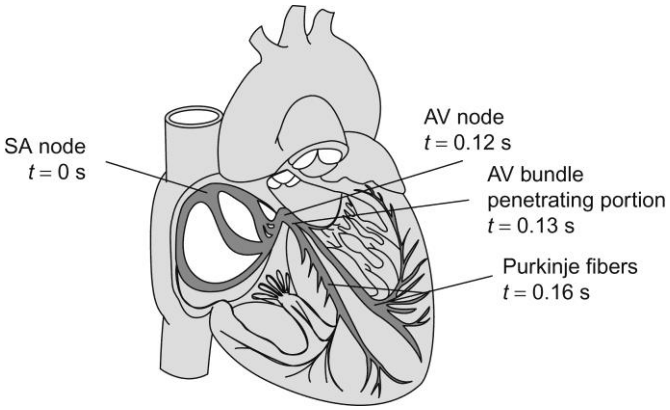

Figure 4.8 SA node and the Purkinje fiber system of the heart, showing the approximate times when the action potential signal reaches various locations within the conducting system. This conducting system allows for a rapid transmission of the cardiac action potential to each cardiac myocyte. For ease of viewing the interatrial band has been removed. This pathway conducts the action potential from the SA node to the left atrium rapidly.

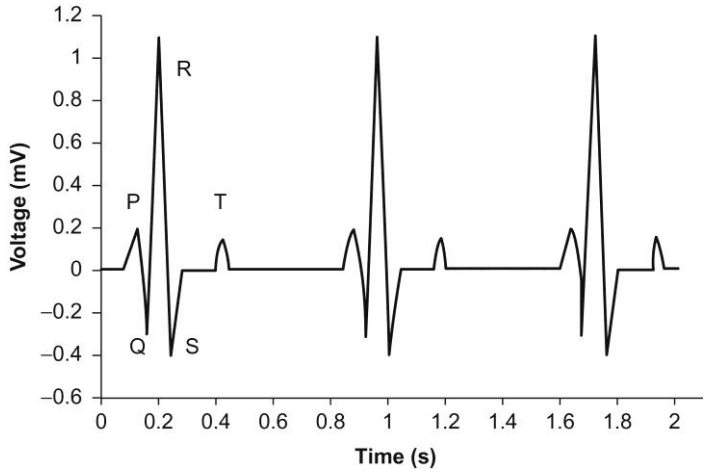

Figure 4.9 Schematic of a normal ECG trace, depicting the various waveforms used to determine if the heart is functioning properly. The P wave is associated with atria contraction, the QRS complex is associated with ventricular contraction, and the T wave is associated with ventricular repolarization. Atrial repolarization is masked by the much larger QRS complex.

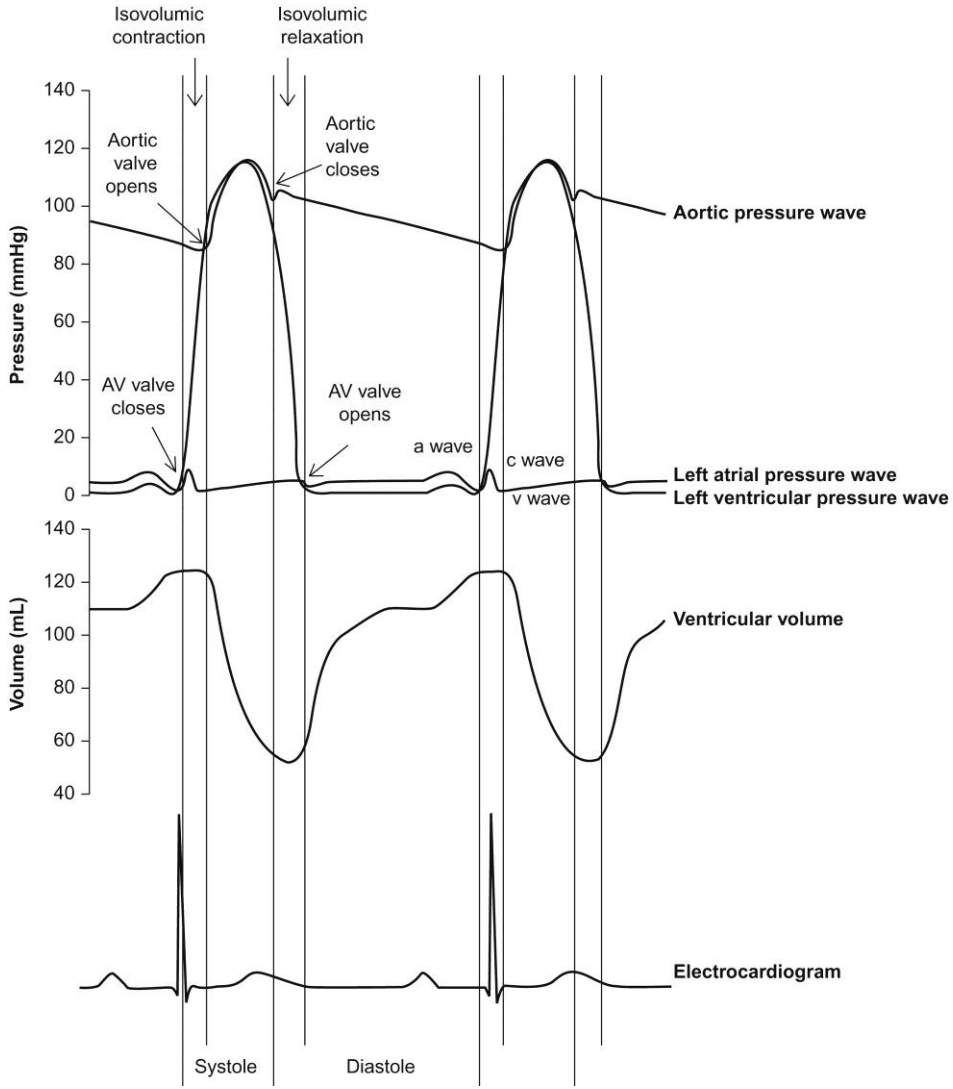

Figure 4.10 Pressure and volume waves associated with the left side of the heart. This figure depicts the relationship between the ECG and the contraction and filling of the cardiac tissue. Various important points are noted such as valve opening and ventricular systole versus ventricular diastole. The named waves that are observed during the atrial waveform are also shown in this figure.

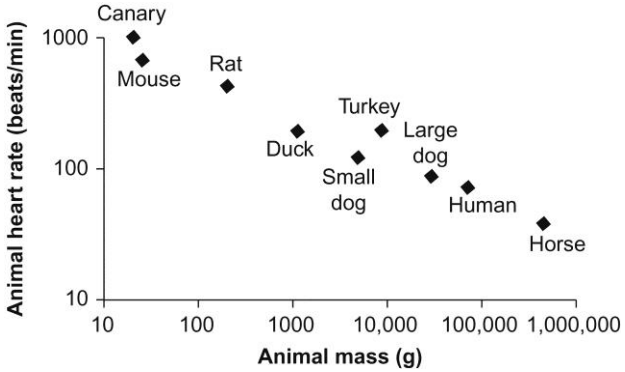

Figure 4.11 The relationship between animal mass and heart rate. As the mass of the animal increases, there is a general decrease in heart rate. The relationship between these two measurements can be correlated to many different properties of the animal, as described in the text.

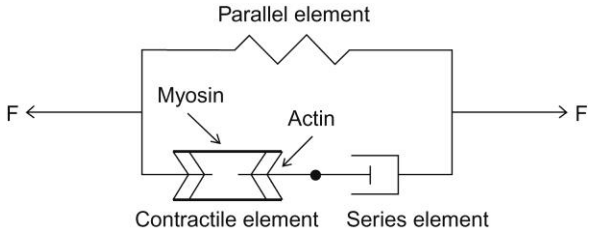

Figure 4.12 A.V. Hill's model for heart muscle contraction, which couples the active contraction component (actin–myosin cross-bridge formation), a viscoelastic relaxation, and a parallel elastic resistance to motion. This is perhaps the most often used model of cardiac muscle contraction and has many forms of quantification.

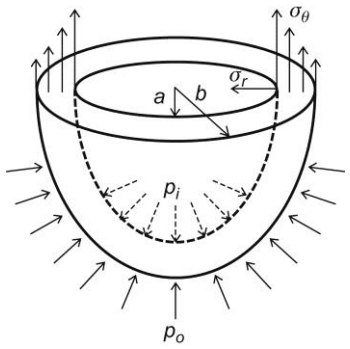

Figure 4.13 Schematic of the radial and circumferential stress in the left ventricle. This assumes that the cardiac tissue is homogeneous in size (and a perfect cylindrical shell) and homogeneous in mechanical properties, and that the pressure loading conditions are uniform. These formulations also neglect the blood flow through the ventricles. Note that we have tried to depict that the circumferential stresses act into and out of the paper, whereas the radial stresses act towards (or away from) the center of the sphere.

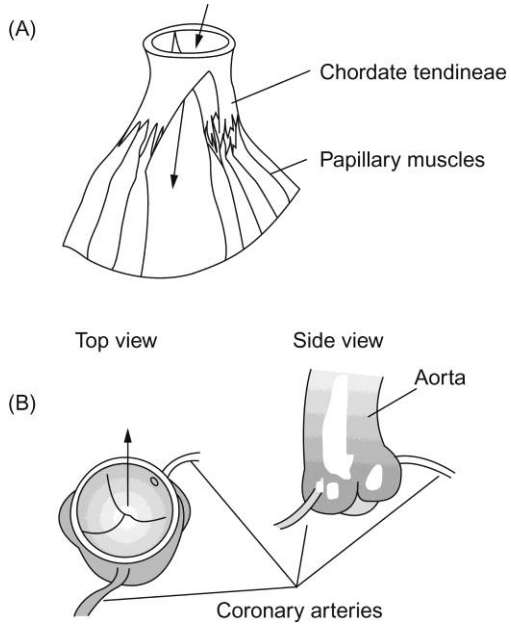

Figure 4.14 The mitral valve (A) and the aortic valve (B) determine the blood flow characteristics and blood flow direction through the left side of the heart. The chordae tendineae and the papillary muscles do not open or close the mitral valve, but instead prevent the leaflets from bulging into the atria during ventricular contraction. The coronary arteries come off the aortic valve sinuses and feed the cardiac tissue with blood. As described in Section 4.6, the flow through the coronary circulation opposes normal flow.

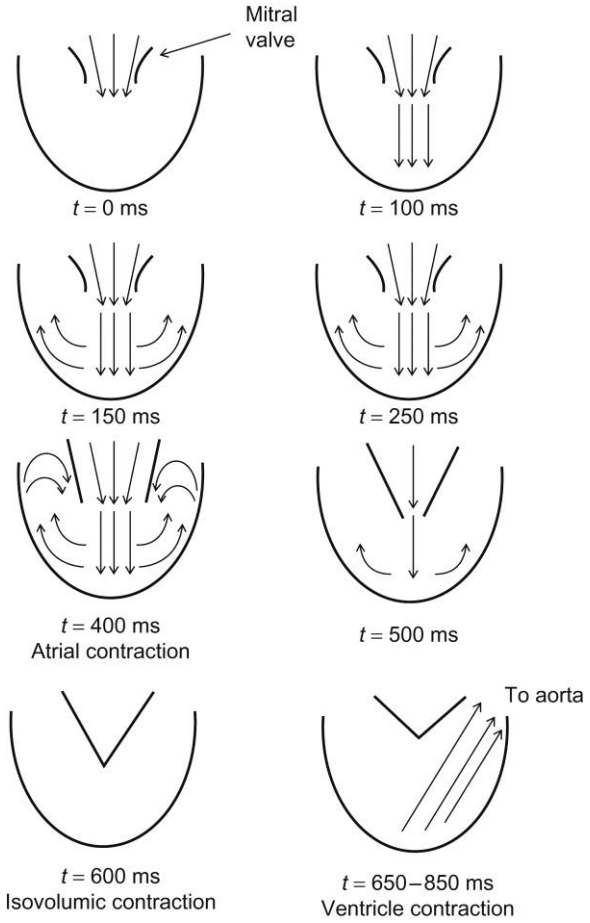

Figure 4.15 Schematic of blood flow through the mitral valve during the cardiac cycle (the papillary muscles/chordae tendineae are not shown). The times shown are approximate, but depict the relative change in blood flow characteristics with time. Note that the blood flow through the mitral valve is largely laminar, even though there is some mixing that may occur behind the valve leaflets.

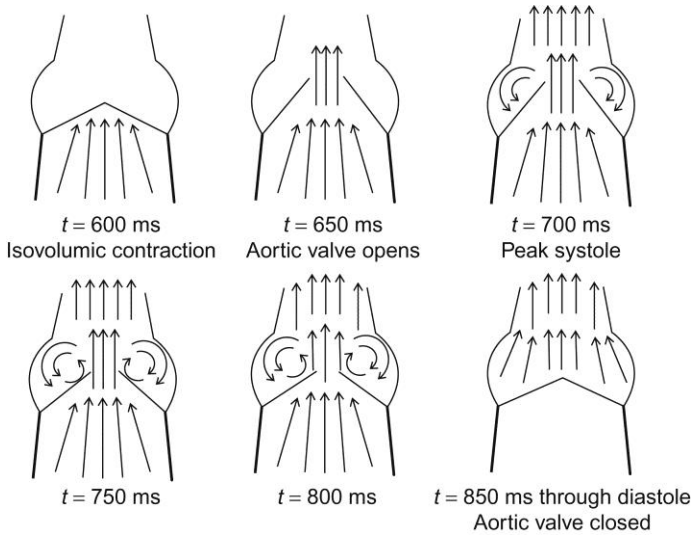

Figure 4.16 Schematic of blood flow through the aortic valve during the cardiac cycle (the times overlap and continue from Figure 4.15). Again, the times are relative, but give a general idea of blood flow through the aortic valve. Again, the flow may approach turbulence through the aortic valve, but this turbulent flow is not self-sustaining and would dissipate instantaneously.

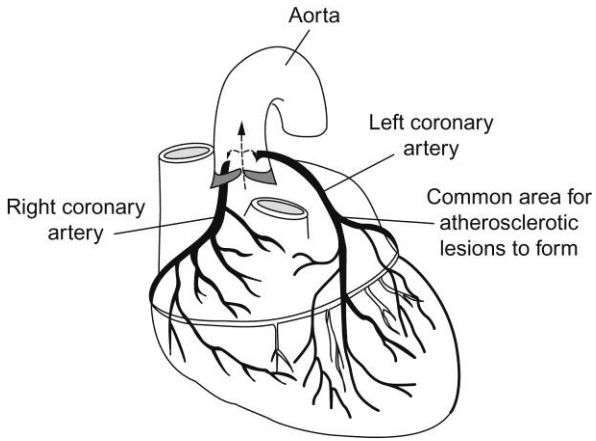

Figure 4.17 The coronary arteries that supply the entire cardiac muscle with blood. These vessels are principal locations for atherosclerotic lesions and other cardiac diseases. Depending on the severity of the damage to these vessels, blood flow to the cardiac muscle cells can be severely impaired.

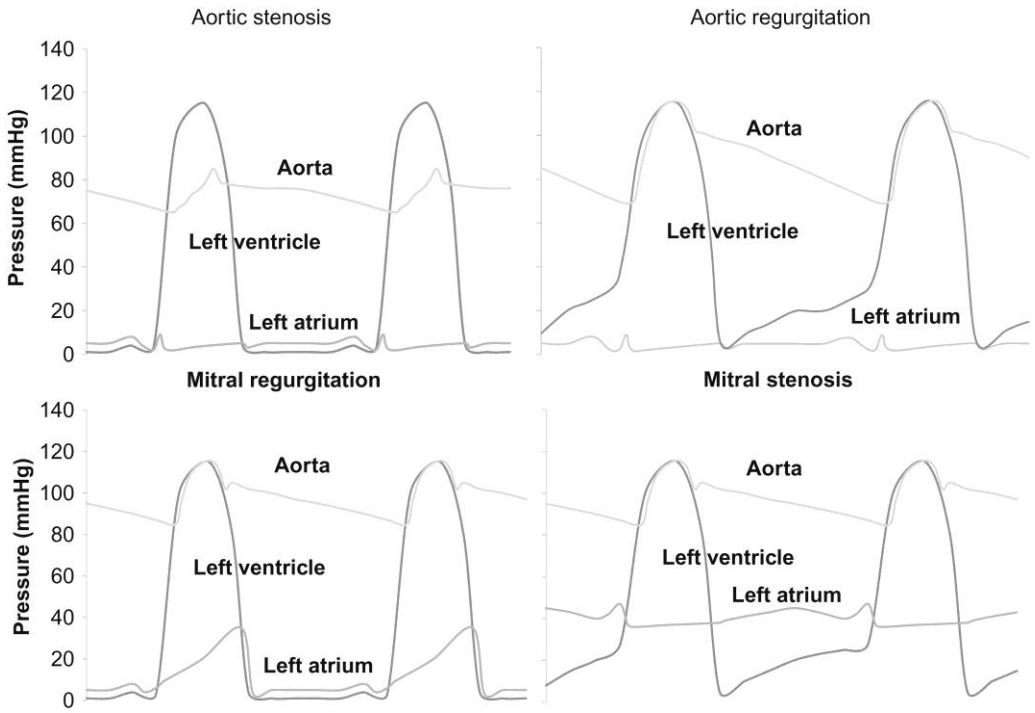

Figure 4.18 Pressure relationship in the left side of the heart and in the aorta during valve diseases of the left side of the heart. The normal relationship for the pressure waveforms can be found in Figure 4.10. The pathologies associated with aortic stenosis (aorta pressure reduction) and mitral regurgitation (left atrium pressure increase) are predominately observed during ventricular systole, whereas the pathologies associated with aortic regurgitation (left ventricle pressure increase/aortic pressure decrease) and mitral stenosis (left atrium pressure increase/left ventricle pressure increase) are predominately observed during ventricular diastole.